COBEM 2023 27TH INTERNATIONAL CONGRESS OF MECHANICAL ENGENEERING

ABCM Brazilian Society of Mechanical Sciences and Engineering
27th ABCM International Congress of Mechanical Engineering
December 04-08, 2023, Florianópolis-SC, Brazil

# COB-2023-0082 – NONLINEAR DYNAMICS OF THE CHAOTIC PENDULUM COUPLED TO A DC MOTOR AND A DC GENERATOR

**Rafael Henrique Avanço**
**Rodrigo Borges Santos**
**Clivaldo Oliveira**
Universidade Federal da Grande Dourados
*rafaelavanco@ufgd.edu.br*
*rodrigobsantos@ufgd.edu.br*
*clivaldooliveira@ufgd.edu.br*
**Maurício A. Ribeiro**
**Angelo Marcelo Tusset**
Universidade Tecnológica Federal do Paraná
*mau.ap.ribeio@gmail.com*
*a.m.tusset@gmail.com*
**Jose Manoel Balthazar**
Universidade Estadual Paulista – Campus de Bauru
*jmbaltha@gmail.com*
**Sanderson Manoel da Conceição**
Universidade Federal da Grande Dourados
*sandersonconceicao@ufgd.edu.br*

***Abstract:*** *The present paper focuses on the dynamics of a pendulum coupled to a DC generator and on the comparison to the parametric pendulum and a pendulum coupled to a DC motor. It is known that a DC generator is a DC motor working on its inverted function. Therefore, different conditions are analyzed duo to the purpose of energy generation. A pendulum vertically vibrated by sea waves can oscillate and rotate. These types of motion in the pendulum can spin the axis of a DC generator and consequently generate energy. The types of motion for the pendulum include stable oscillation, stable rotation, and tumbling chaos. The results with stable rotation are the most desirable, considering it will produce a sinusoidal voltage. The presence of chaos is verified by Lyapunov exponents and Poincare sections. Time histories and phase portraits demonstrate appropriately the kinds of motion obtained. Bifurcation diagrams allow to find the frontiers for the pendulum motion type. Models obtained for the different situations are based on dimensionless parameters relating mechanical and electrical values. A complete analysis of the results leads to where is the range for the amplitude and frequency of excitation that can provide energy harvest from the sea waves. In the ideal motion, we consider the amplitude as an imposed parameter and in the nonideal the displacement in the pendulum and the frequency are a consequence of the voltage set in the DC motor. In the results, where the DC generator is spined by the pendulum, the amplitude and frequency are obtained by the sea waves moving the pendulum and consequently generating energy.*

***Keywords:*** *Pendulum, DC Generator, DC motor and Energy Harvesting*

## 1. INTRODUCTION

The classic parametric pendulum is vastly studied in literature duo to scientific interest in chaotic results, but recently the technological usage of the pendulum in energy harvest is gaining visibility. The present paper focus on simulating the dynamics of a pendulum coupled to a DC generator and compare to the results present in literature for the classic parametric pendulum and the pendulum coupled to a DC motor. A DC motor and the classic parametric pendulum produces similar types of motion for the pendulum vibrated. The classic parametric pendulum exhibits: stable oscillations, stable rotations, fixed point (the pendulum at rest), stable oscillations with rotations and the tumbling chaos. When the pendulum is under tumbling chaos, it rotates and oscillates unpredictably. This chaotic motion is frequently verified using Poincare sections with the presence of a strange attractor demonstrating a fractal appearance. The presence of chaos is also verified by Lyapunov exponents, where a useful algorithm is demonstrated in Wolf et al. (1985).

The chaos in the classic parametric pendulum was first explored in Leven and Koch (1981) with Lyapunov exponents verifying the presence of chaotic motion. In the sequence, rotating orbits were analyzed in Xu et al. (2005) mentioning the idea of the energy harvest from sea waves but still without a mechanism included in the dynamic model.

In Nandakumar et al. (2012), the analysis explores an optimum energy extraction from rotational motion of the parametric pendulum and in Avanço et al. (2019) a modeling of a pendulum coupled to a generator was presented, whist in Avanço et al. (2018) a pendulum vibrated in the horizontal direction by a DC motor was studied.

## 2. DYNAMICAL MODELING

The dynamics of the pendulum is determined by Lagrange equations derived accordingly the generalized coordinates. For the ideal vibration the unique coordinate is the pendulum angle α. For the nonideal vibrations with a pendulum and a DC motor, the coordinates are the pendulum angle α and the motor angle θ. When there is a DC generator coupled to the pendulum, they rotate at the same speed in our mechanism, so there is only one generalized coordinate.

### 2.1 Ideal vibration of the pendulum

The model of an ideal vibration of the pendulum is the same of the classic parametric pendulum. It is the same model present in Leven and Koch (1981), Xu et al. (2005) and Avanço et al. (2016). The apostrophe in the Eq. (1) represents a derivative related to the dimensionless time τ. The dimensionless damping is represented by $\gamma$. The symbol ω is the dimensionless frequency and $p$ is related to both amplitude and frequency. In Eq. (2) the terms in the left-hand side of equations are all dimensionless. The right-hand side of equations have the terms Ω equal to the frequency of excitation, $\omega_0$ the natural frequency of the pendulum, $m$ is the mass of the pendulum, $c$ is the viscous friction of the pendulum, $l$ is the length of the pendulum and $a$ is the amplitude of the excitation.

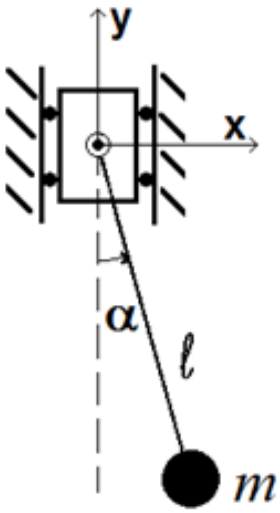


Figure 1. The classic parametric pendulum

$$\alpha'' + \gamma\,\alpha' + \sin\alpha\ (1 + p\cos(\omega\tau)) = 0 \tag{1}$$

The dimensionless terms are present in Eq. (2), where $a$ is the amplitude of excitation.

$$\begin{aligned} \omega &= \frac{\Omega}{\omega_0} \\ p &= \frac{a}{l}\omega^2 \\ \gamma &= \frac{c}{m\,\omega_0} \\ \tau &= \omega_0 t \end{aligned} \tag{2}$$

### 2.2 Nonideal vibration of the pendulum

The nonideal vibration of the pendulum linked to the DC is modeled in a similar way. The Lagrangian equations are obtained deriving the generalized coordinates α and θ. Instead of Ω the excitation speed is given by the motor speed $\dot{\theta}$ where the dot is a derivative related to the physical time $t$. The term $a$ is the radius of the crank while $b$ is the length of the shaft. The dynamic model in this subsection is similar to that presented in Avanço et al. (2019).

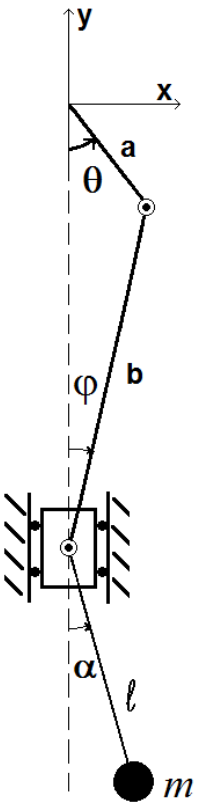


Figure 2. The crank slider mechanism powered by the DC motor.

The coordinates $x$ and $y$ are the position of the pendulum considering the reference of the center of the crank.

$$x = l\sin\alpha$$
$$y = -acos\theta - bcos\varphi - lcos\alpha \tag{3}$$

The term $\varphi$ is the angle of the shaft which has its relation to the angle $\theta$ present in the Eq.(4).

$$\cos\varphi = \left(1 - \frac{a^2}{b^2}sin^2\theta\right)^{1/2} \tag{4}$$

Considering the Kinect and potential energy the Lagrangian function is written in Eq.(5) where J represents the rotor inertia, g is the gravitational acceleration and $F$ is an auxiliary function:

$$L_a = \frac{1}{2}J\dot{\theta}^2 + \frac{1}{2}m\left(l^2\dot{\alpha}^2cos^2\alpha + \left[a\dot{\theta}F + l\dot{\alpha}sin\alpha\right]^2\right) + mglcos\alpha + mgb\left(1 - \frac{a^2}{b^2}sin^2\theta\right)^{1/2} + mgacos\theta \tag{5}$$

This auxiliar function F is described in Eq. (6) and it will be used in the next equations.

$$F = sin\,\theta + \frac{a\,sin\,\theta\cos\theta}{b\left(1 - \frac{a^2}{b^2}sin^2\theta\right)^{1/2}} \tag{6}$$

The final differential equation derived by the coordinate α is given by Eq (7). It is important to observe the apostrophe means a derivative related to the dimensionless time $\tau$.

$$\alpha'' + \gamma\alpha' + \frac{a\,sin\,(\alpha)F\theta''}{l} + \frac{a\,sin(\alpha)F'\theta'}{l} + sin(\alpha) = 0 \tag{7}$$

The differential equation for the motor speed is found when one derives the Langrangian function in relation to the coordinate θ. This differential equation is in the Eq. (8), where $M_{motor}$ is the torque supplied by the DC motor and $c_m$ is the viscous friction in the center of this motor:

$$J\omega_0\theta'' + ma^2F^2\omega_0^2\theta'' + ma^2FF'\theta'\omega_0^2 + maFl\cos(\alpha)\ \omega_0^2\alpha'^2 + maFl\ sen(\alpha)\omega_0^2\alpha'' + mgaF = M_{motor} - c_m\theta'\omega_0 \quad (8)$$

Torque supplied by the motor is presented by the Eq. (9), where the terms $K_T$ represents the constant of torque, $K_E$ the electrical constant, $R$ the internal resistance of the armature and $V$ is the Voltage set.

$$M_{motor} = \frac{K_T V}{R} - \frac{K_E K_T}{R}\ \omega_0\theta' \quad (9)$$

Following the equations Eq. (7), Eq. (8) and Eq. (9) it is completed the aim to model this nonideal vibration problem. The results from the nonideal problem approaches to ideal when the power generated by the motor is much higher to the consumed. It is also possible to affirm that the higher is the length of $b$ more this model approaches to the pendulum vibrated by harmonic vertical excitation.

### 2.3 Pendulum coupled to the generator

The pendulum coupled to the generator have the property of both rotate at the same speed. Therefore, this model is very similar to the ideal model of pendulum vertically vibrated by a harmonic movement and it is similar to that in Avanço et al (2019). Using a DC generator, it is inserted a new differential equation present in Eq. (10). The term $L$ represents the inductance the generator, $R_L$ is the resistance of the inductor and $R_a$ any other resistance and the term $i$ is the electric current.

$$L\ \frac{di}{dt} = -(R_a + R_L)i + K_E\dot{\alpha} \quad (10)$$

Using the dimensionless parameters in Eq. (11) it is possible to lead the system to a set of differential equations. Equation (12) represents the nondimensional electric equation of the DC generator and the Eq. (13) represents the dynamical equation of the pendulum motion. In Eq. (11) the term I stands for the dimensionless current while the term $i$ is the real current. The obtainment of this relation is based on the natural frequency of the pendulum $\omega_0$ and an arbitrary electric charge Q. It is suggested this electric charge Q to be equal to the elementary charge $1.6 \cdot 10^{-19}C$.

$$\beta = \frac{K_T Q}{ml^2\omega_0}\quad I = \frac{i}{Q\omega_0}\quad \lambda = \frac{K_E}{Q\omega_0 L}\quad \zeta = \frac{(R_a + R_L)}{\omega_0 L} \quad (11)$$

$$\frac{dI}{d\tau} = -\zeta\, I + \lambda\, \alpha' \quad (12)$$

$$\alpha'' + \gamma\alpha' + sin\ \alpha\ (1 + p\ cos(\omega\tau)) + \beta I = 0 \quad (13)$$

## 3. RESULTS

The results demonstrated from Figure 3 to Figure 9 are all related to the model present in the section 2.3 for the pendulum coupled to the generator. Comparing these results to the results presented for the classic parametric pendulum in Avanço et al. (2016) and to the results for the DC motor in Avanço et al. (2019), it is possible to affirm the resonance zones occur for the frequencies ω equal to 1.8 and 0.9 for these three models in the conditions analyzed.

In Figure 3, there is a bifurcation diagram for the parameter p from 0 to 4. This same range is analyzed by Lyapunov exponents where positive values indicate chaotic results. Comparing the bifurcation diagram and Lyapunov exponents in Figure 3, it is possible to conclude that they agree when someone is looking for the chaotic region.

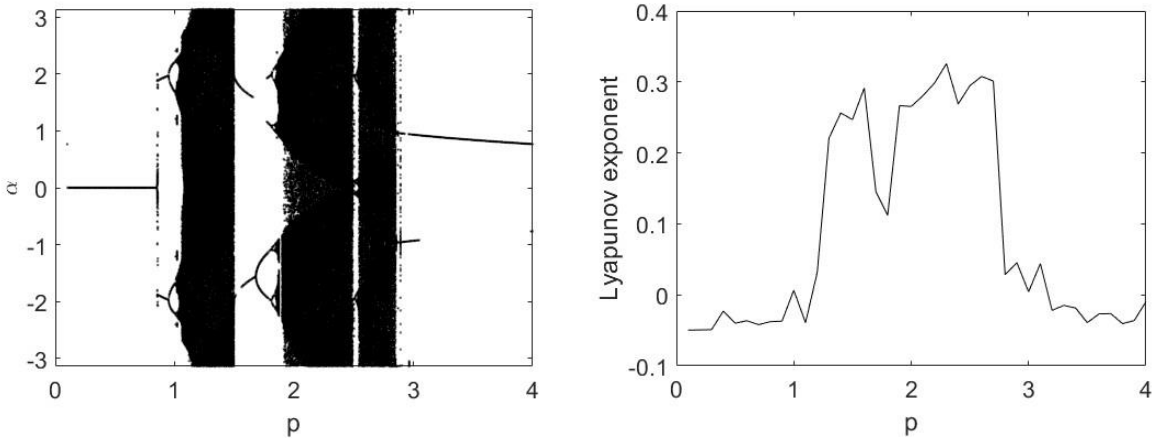


Figure 3. (a) The bifurcation diagram and (b) The Lyapunov exponents for $\omega$=1.8, λ=0.3, β=1.0 and $\zeta = 1.0$

From the bifurcation diagram in Figure 3, it was chosen different values of p and Poincare section were used to discover the types of motion involved. Times histories of the pendulum angle and the phase portrait were also useful.

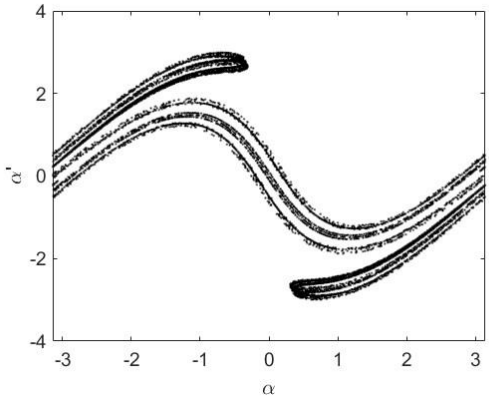


Figure 4. Poincare section for p=2.1, $\omega$=1.8, λ=0.3, β=1 and $\zeta$ =1

The Poincare section from Figure 4 demonstrates a chaotic motion in the main resonance zone and its time history of the angle with the phase portrait are present in Figure 5. In order to plot results in the interval -π to π, the angles had the laps subtracted to keep this interval in the Poincare sections and phase portraits. Time histories maintain its real angle.

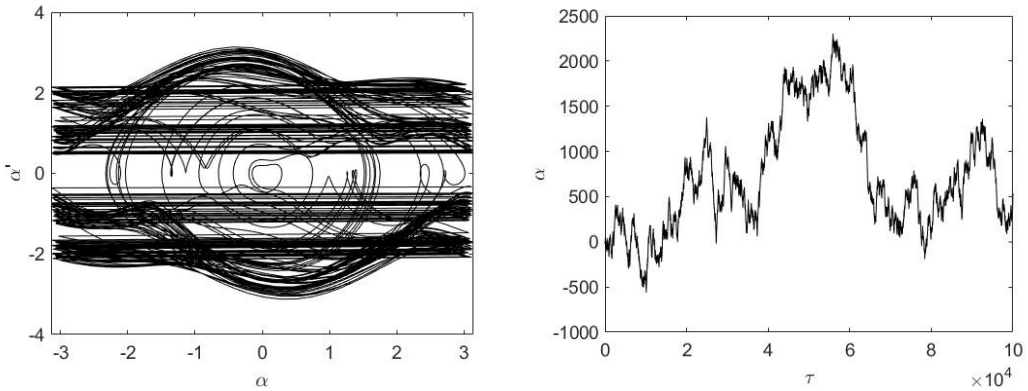


Figure 5. Phase portrait and Time history for the pendulum for the parameters p=2.1, $\omega$=1.8, λ=0.3, β=1 and $\zeta$ =1

Still in the main resonance zone it is found a period-1 rotation is represented for $p$ equal to 3.5 in the Figure 6 where the time history and phase portrait demonstrate the rotation of the pendulum but without the Poincare section. The Poincare section was not necessary because the bifurcation diagram is enough for concluding it was a period-1 motion.

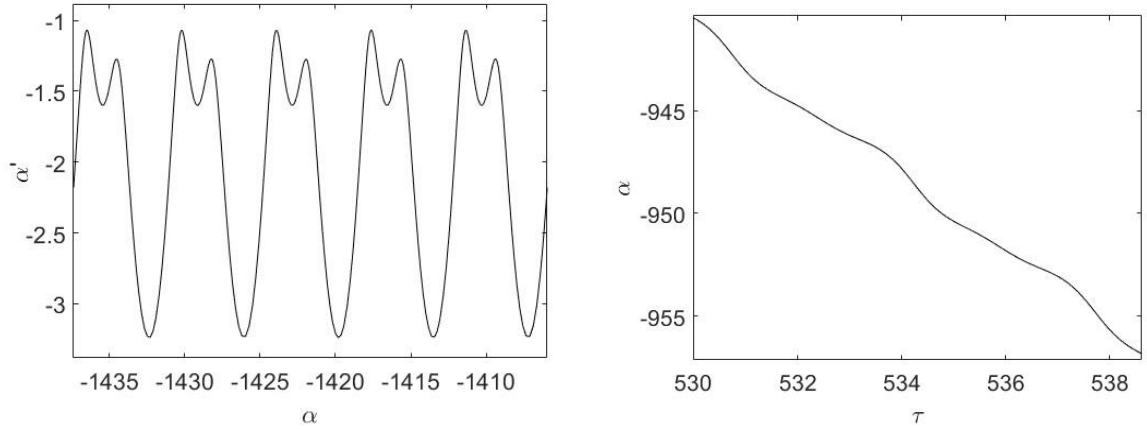


Figure 6. Phase portrait and Time history for the pendulum for the parameters p=3.5, $\omega$=1.8, λ=0.3, β=1 and $\zeta$ =1

In the Figure 7, there are two graphics with bifurcation diagram and Lyapunov exponents for a subharmonic resonance. For these results the frequency used was ω equal to 0.9 and the other parameters used were the same as the previous. The zones were Lyapunov exponents point chaos are the same zone where the bifurcation diagrams indicate the chaos.

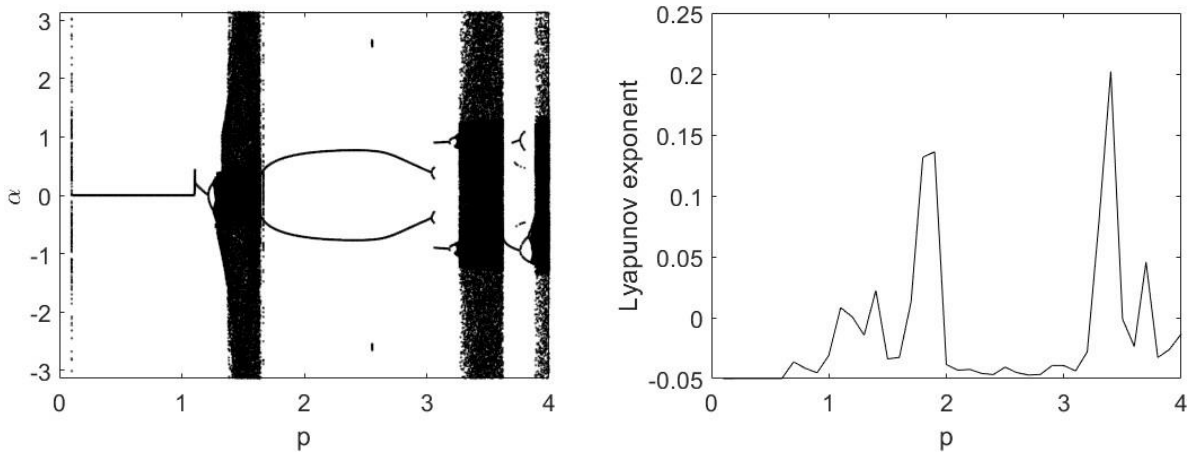


Figure 7. (a) The bifurcation diagram and (b) The Lyapunov exponents for $\omega$=0.9, λ=0.3, β=1.0 and $\zeta = 1.0$

Different kinds of motion are found for the pendulum in this subharmonic resonance. A 2-period oscillatory motion is in Figure 8 with the Poincare section and in Figure 9 with the Phase portrait and time history for $p$ equal to 2.0 and ω equal to 0.9 in this subharmonic resonance.

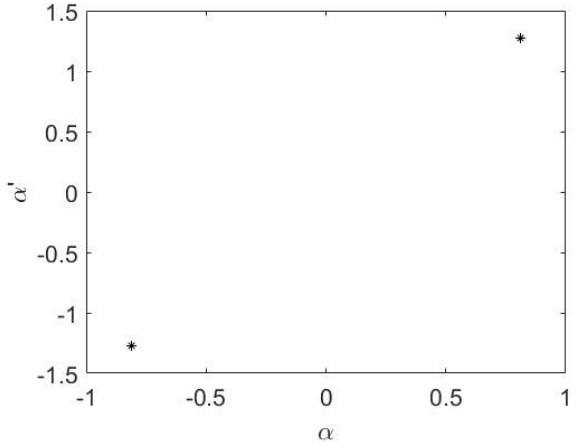


Figure 8. Poincare section for 2-period oscilation p=2.0; $\omega$=0.9, λ=0.3, β=1.0 and $\zeta = 1.0$

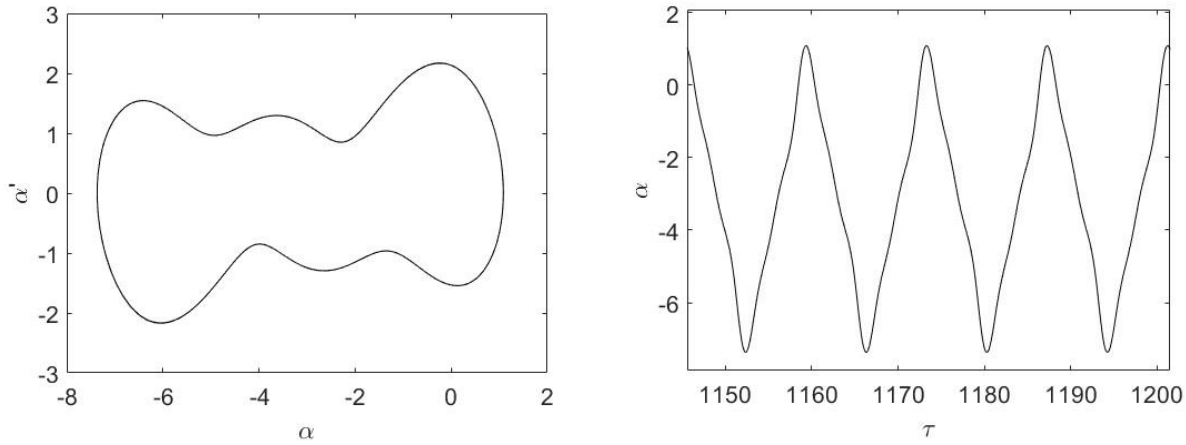


Figure 9. (a) Phase portrait and (b) Time history for oscillation with p=2.0; $\omega$=0.9, λ=0.3, β=1.0 and $\zeta = 1.0$

## 4. CONCLUSION

The pendulum coupled to the DC generator exhibits different types of motion for the pendulum, including fixed points, oscillation, rotation, oscillations with rotations, and chaos. They are the same types of motion present in the literature for the pendulum vibrated by the DC Motor and the classic parametric pendulum. As expected, differences appear in the bifurcation diagrams with shifts in the types of motion dependent on dimensionless parameters. Despite these shifts, the resonance zone keeps the same the present for the DC motor and the ideal excitation of the pendulum. The resonance zone was verified for $\omega$ equal to 1.8 and 0.9. For future works it is suggested that it would be useful to increase the range of analysis for the parameters and include some parameters plot demonstrating the different types of motion for the parameters $\omega$, $p$, λ, β and $\zeta$.

## 5. REFERENCES

Avanço, R.H., Navarro,H.A., Brasil, R.M.L.R.F., Balthazar, J.M., Bueno, A.M., Tusset, A.M. (2016) Statements on nonlinear dynamics behavior of a pendulum, excited by a crank-shaft-slider mechanism, Meccanica 51, 1301-1320.

Avanço, R.H., Tusset, A.M., Balthazar, J.M., Nabarrete, A., Navarro, H.A. (2018) On nonlinear dynamics behavior of an eletro-mechanical pendulum excited by a nonideal motor and a chaos control taking into account parametric errors. Journal of Brazilian Society of Mechanical Sciences and Engineering 40, article 23.

Avanço, R.H., Tusset, A.M., Suetake, M., Navarro, H.A., Balthazar, J.M., Nabarrete, A. (2019) Energy Harvesting through pendulum motion and DC generators. Latin American Journal of Solids and Structures.

Leven, R.W., Koch, B.P. (1981) Chaotic Behavior of a Parametrically-Excited Pendulum, Physics Letters A, vol.86, n.2, November 2nd 1981.

Nandakumar, K., Wiercigroch, M., Chatterjee, A. (2012) Optimum energy extraction from rotational motion in a parametrically excited pendulum, Mechanics Research Communications, Volume 43, 2012, Pages 7-14, ISSN 0093-6413.

Wolf, A., Swift, J.B., Swinney, H.L., Vastano, J.A. (1985) Determining Lyapunov Exponents from a Time Series, Physica D, vol 16, pp. 285-317.

Xu, X., Wiercigroch, M., Cartmell, M.P. (2005) Rotating Orbits of a Parametrically-excited Pendulum. Chaos, Solitons and Fractals, v.23, pp. 1537-1548, 2005.

## 6. RESPONSIBILITY NOTICE

The author(s) is (are) the only responsible for the printed material included in this paper.